



Optical Materials

Guide for Authors ▼

Submit Your Paper ▼

Track Your Paper ▼

Order Journal

View Articles

Journal Insights

Open Access Options

Most Downloaded
ArticlesRecent Open Access
Articles

News

Most Cited Articles

Special Issues

Recent Articles

Stay up-to-date

Register your interests
and receive email alerts
tailored to your needs

[Click here to sign up](#)

Follow us



Most Downloaded Optical Materials Articles

The most downloaded articles from [ScienceDirect](#) in the last 90 days.

1. Properties of transparent Ce:YAG ceramic phosphors for white LED

March 2011

S. Nishiura | S. Tanabe | K. Fujioka | Y. Fujimoto

Abstract: Transparent Ce:YAG ceramic phosphors were synthesized from the oxide powder which was produced by co-preparation method of the hydroxides. The Ce:YAG ceramics had a broad emission band peaked at 530nm due to the 5d→4f transition of Ce³⁺. The transmittances of the samples obtained were 70–87% at 800nm. The absorption coefficient and emission intensity of Ce³⁺ were increased with increasing thickness. Under 465nm LED excitation, the color coordinates of the Ce:YAG ceramics shifted from the blue region to yellow region with increasing sample thickness, passing nearby the theoretical white point in the chromaticity diagram. The highest value of luminous efficacy of the ceramic white LED was 73.5lm/W.

Share Article



2. Analysis of the dispersion of optical plastic materials

July 2007

Stefka Nikolova Kasarova | Nina Georgieva Sultanova | Christo Dimitrov Ivanov | Ivan Dechev Nikolov

Share Article



3. A review on the light extraction techniques in organic electroluminescent devices

November 2009

Kanchan Saxena | V.K. Jain | Dalip Singh Mehta

Abstract: Organic electroluminescent devices are becoming increasingly important because of their potential applications for large area flat-panel displays and general lighting. The internal quantum efficiency of these devices have been achieved near 100% using electro-phosphorescent materials with proper management of singlet and triplet excitons, however, the external quantum efficiency of conventional devices remains near 20% because of losses due to wave-guiding effect. Recently, there has been great progress to enhance the light out-coupling efficiency of organic electroluminescent devices by means of various internal and external device modification techniques. In this review we report recent advances in light out-coupling techniques, such as, substrate modification methods, use of scattering medium, micro-lens arrays, micro-cavity effect, photonic crystals and nano-cavity, nano-particles, nano-structures and surface plasmon-enhanced techniques that have been implemented to enhance the external extraction efficiency of organic electroluminescent devices.

Share Article



4. Novel materials doped with trivalent lanthanides and transition metal ions showing near-infrared to visible photon upconversion

March 2005

J.F. Suyver | A. Aebischer | D. Biner | P. Gerner | J. Grimm | S. Heer | K.W. Krämer | C. Reinhard | H.U. Güdel

Abstract: This paper presents an overview of the recent results on upconversion spectroscopy obtained in our group. After a brief introduction into the upconversion field, three different topics will be addressed. First, the near-infrared (NIR) to red/green or blue upconversion efficiencies are discussed for the very efficient upconversion lattice NaYF₄ codoped with Er³⁺, Yb³⁺/Er³⁺ or Yb³⁺/Tm³⁺, respectively. It will be demonstrated that as much as 50% of the NIR excitation photons contribute to the upconversion emission. Possible application of such a phosphor for enhancing the energy conversion efficiency of solar cells will be discussed. Next, the upconversion spectroscopy of nanocrystalline solutions will be discussed. Most importantly, optically transparent solutions showing intense visible emission under near-infrared excitation, an essential first step for application in new luminescent nanolabels, will be presented. Finally, upconversion spectroscopy of mixed transition metal/rare earth systems will be discussed. Both systems where the sensitizer is the rare earth ion and upconversion occurs on the transition metal ion, and their counterparts (transition metal sensitized upconversion) are presented and their underlying mechanisms will be described. The possibilities for chemical tuning of upconversion properties in such systems are presented.

Share Article



5. Bright orange upconversion in a ZnO–TiO₂ composite containing Er³⁺ and Yb³⁺

January 2014

Hom Nath Luitel | Kazuya Ikeue | Risa Okuda | Rumi Chand | Toshio Torikai | Mitsunori Yada | Takanori Watari

Abstract: ZnO–TiO₂ composite system containing Er³⁺ and Yb³⁺ were prepared by solid state reaction method and its upconversion (UC) luminescence excited by 980nm laser was studied for the first time. The effects of firing temperature, ZnO/TiO₂ composition and Er³⁺, Yb³⁺ concentrations on the UC emission behavior were examined. The ZnO–TiO₂ composite product sintered at 1200°C contained Zn₂TiO₄, TiO₂ and RE₂Ti₂O₇ (RE=Er³⁺ and Yb³⁺) phases and exhibited strong green and red emissions arising due to the 2H_{11/2}, 4S_{3/2}→4I_{15/2} and 4F_{9/2}→4I_{15/2} transitions for Er³⁺ ion, respectively. Bright orange color by the mixing of green and red colors was observed in the 1ZnO–1TiO₂ product doped with 2at.% Er³⁺ and 6at.% Yb³⁺. The ZnO–TiO₂:Er³⁺, Yb³⁺ phosphor was compared to the brightest available phosphor, Y₂O₃:Er³⁺, Yb³⁺ and found to be 3-fold brighter than it. It suggests that ZnO–TiO₂:Er³⁺, Yb³⁺ is a potential material for the orange upconversion phosphor.

Share Article



6. Blue organic light emitting materials: Synthesis and characterization of novel 1,8-naphthalimide derivatives

January 2014

Hidayath Ulla | B. Garudachari | M.N. Satyanarayan | G. Umesh | A.M. Isloor

Abstract: A series of naphthalimide derivatives were designed and synthesized by substituting electron-donating phenoxy groups at the 4th position of 1,8-naphthalimide. Photophysical, thermal, electrochemical properties of the synthesized derivatives were studied. The photophysical studies revealed that by varying the substituents at the 4th position of the 1,8-naphthalimide backbone, the photoluminescence spectra can be readily tuned in the range 410–423nm (solution) and 457–468nm (thin film). The derivatives have high Stokes' shifts and the Commission Internationale de l'Eclairage (CIE) coordinates are positioned in the deep blue region of the chromaticity diagram. Thermal analysis showed that the melting points are in the range 135–270°C with good thermal stability of 260–275°C. Electrochemical studies show the derivatives to have low-lying energy levels revealing that they possess good electron-transporting and hole-blocking properties. The ionization potentials and electron affinity are in the region of 6.30–6.36eV and 3.31–3.43eV, respectively, with energy band-gaps in the range 2.93–3.0eV. The studies reveal that these energy values are relatively higher than the commonly used electron transporting materials. Hence these derivatives are potential candidates not only as electron transporting but also as hole blocking blue emitters for organic light-emitting diode applications.

Share Article



7. Highly conductive and transparent reduced graphene oxide/aluminium doped zinc oxide nanocomposite for the next generation solar cell applications

December 2013

Ian Y.Y. Bu

Abstract: In this paper, aluminum-doped zinc oxide(AZO)/reduced graphene oxide nano-composite thin films are synthesized by a one-pot, solution-processed method. The nanocomposite film has been extensively characterized using scanning electron microscopy (SEM), X-ray-diffraction (XRD), energy dispersive spectroscopy (EDS), Hall effect measurement and UV–Vis spectroscopy. It is found that the controlled addition of reduced graphene oxide into AZO can lower the film's resistivity without causing significant degradation of optical transparency. In addition, nanocomposite films post-annealed at process temperature at 500°C possesses the lowest resistivity and the highest optical transmittance and that further increases in the annealing temperature degrades the film's property due to nucleation of other phases of the AZO.

Share Article



8. Optical and structural characterization of TiO₂ films doped with silver nanoparticles obtained by sol–gel method

December 2013

T. Ivanova | A. Harizanova | T. Koutzarova | B. Vertruyen

Abstract: Nanostructured titanium oxide films with incorporated Ag nanoparticles were deposited by sol–gel spin coating method. The films were annealed at 300°C, 400°C, 500°C and 600°C in oxygen and nitrogen ambient. X-ray diffraction (XRD), Fourier Transform Infrared Spectroscopy (FTIR) and UV–VIS spectroscopy had been applied for studying the influence of the thermal treatments and the gas ambient on the structural and optical properties of TiO₂ and TiO₂:Ag films. The XRD analysis revealed the presence of metallic Ag phase without traces of silver oxides and these results were confirmed by FTIR spectra. It has been revealed that the annealing temperatures and the ambient, where the annealing is carried out is crucial for TiO₂ crystallization, when there is Ag incorporation and especially for appearance of anatase and rutile phase. The nitrogen and oxygen ambient influences quite different the crystallization of TiO₂:Ag films. Transmission and absorption spectra have been analyzed. Optical band gap values were evaluated for pure titania and Ag incorporated TiO₂ films.

Share Article



9. Synthesis and luminescent properties of UV-excited thermal stable red-emitting phosphor Ba₃Lu(PO₄)₃: Eu³⁺ for NUV LED

February 2014

Xinguo Zhang | Jilin Zhang | Menglian Gong

Abstract: A series of Ba₃Lu(PO₄)₃: Eu³⁺ phosphors were synthesized by high-temperature solid-state method, and their UV–vis luminescent properties were investigated. The f–f transitions of Eu³⁺ in the host lattice were assigned and discussed. The excitation and emission spectra indicate that this phosphor can be excited by near ultraviolet (NUV) light, and exhibits strong red emission. The concentration quenching on Eu³⁺ emission and its mechanism were investigated. This phosphor shows a good thermal stability at high temperature (~180°C). The fabricated prototype LEDs with Ba₃Lu(PO₄)₃: Eu³⁺ and 395nm-emitting InGaN chips exhibit bright red emission. The present study suggests that Ba₃Lu(PO₄)₃: Eu³⁺ can be a potential red phosphor for NUV light-emitting diodes.

Share Article



10. Waveguiding properties of a silicon nanowire embedded photonic crystal fiber

March 2014

E. Gunasundari | K. Senthilnathan | S. Sivabalan | Abdosllam M. Abobaker | K. Nakkeeran | P. Ramesh Babu

Abstract: We design a photonic silicon nanowire embedded microstructured optical fiber which is a special class of waveguide whose core diameter is of subwavelength or nanometer size with the air holes in the cladding. We study the optical waveguiding properties, namely, waveguide dispersions, fractional power and effective nonlinearity by varying the core diameter. The results reveal that the air-clad silicon subwavelength nanowire exhibits several interesting properties such as tight-confinement, a large normal dispersion (82,385ps²/km) for 300nm core diameter and a large anomalous dispersion (–6817.3ps²/km) for 500nm core diameter at 1.95μm wavelength. The structure offers two zero dispersions, one at 1.26μm wavelength for a core diameter of 300nm and another at 1.83μm wavelength for 400nm core diameter. Besides, it provides a large nonlinearity (5672.7W^{–1}m^{–1}) at 0.450μm wavelength for 300nm core diameter. These enhanced optical properties might be suitable for various nonlinear applications.

Share Article



11. Photon avalanche upconversion in rare earth laser materials

January 1999

Marie-France Joubert

Abstract: We present an overview of the upconversion mechanisms with special attention to the Photon Avalanche (PA) process and to give the state of the art concerning the upconversion pumped solid state lasers.

Share Article



12. Ceramic laser materials: Past and present

February 2013

Jasbinder Sanghera | Woohong Kim | Guillermo Villalobos | Brandon Shaw | Colin Baker | Jesse Frantz | Bryan Sadowski | Ishwar Aggarwal

Abstract: Recently, 100KW output power from YAG ceramic laser system has been demonstrated. It is a remarkable achievement considering that only a few milli-watt power was observed from the ceramic laser materials when first reported in the 1960s. This great improvement is mainly due to the success in high purity powder synthesis, development in new sintering technology and novel ideas in optics and device design. Additional developments have included highly doped microchip lasers, ultrashort pulse lasers, novel materials such as sesquioxides, fluoride ceramic lasers, selenide ceramic lasers in the 2–3μm region, composite ceramic lasers for better thermal management, and single crystal lasers derived from polycrystalline ceramics. In this paper, we highlight some of these notable milestones and achievements and forecast the future in polycrystalline ceramic laser materials.

Share Article



13. Self-assembled RE₂(MO₄)₃:Ln³⁺ (RE=Y, La, Gd, Lu; M=W, Mo; Ln=Yb/Er, Yb/Tm) hierarchical microcrystals: Hydrothermal synthesis and up-conversion luminescence

January 2014

You Zhou | Xiang-Hong He | Bing Yan

Abstract: RE₂(MO₄)₃:Ln³⁺ (RE=Y, La, Gd, Lu; M=W, Mo; Ln=Yb/Er, Yb/Tm) microstructures with uniform shapes and sizes were synthesized via a hydrothermal method in the presence of hexadecyl trimethyl ammonium bromide (CTAB). The structure and morphology of the as-prepared microcrystals were characterized by X-ray diffraction (XRD), scanning electron microscopy (SEM), transmission electron microscopy (TEM), selected area electron diffraction (SAED) and high-resolution transmission electron microscopy (HRTEM). The 3D hierarchical architectures of Y₂(MoO₄)₃:Yb³⁺/Er³⁺ and

Gd₂(WO₄)₃:Yb³⁺/Er³⁺ are self-assembled by numerous nanoflakes. The up-conversion (UC) luminescence properties of these samples were investigated. Obvious differences in up-converted emission spectra among the as-obtained products were observed, and possible reasons were discussed. The corresponding up-conversion mechanism was also proposed.

Share Article



14. An alternative description for the interaction between the Eu³⁺ ion and its nearest neighbours

January 2014

Y.A.R. Oliveira | H. Lima | A.S. Souza | M.A. Couto dos Santos

Abstract: The LiYF₄:Eu³⁺ and the Eu(btfa)₃(4,4-bipy)(EtOH) compounds are being revisited by the method of equivalent nearest neighbours (MENN) and the simple overlap model, this time to suggest a comparison between the europium local symmetry in complexes containing β-diketones and the S₄ symmetry in the LiYF₄:Eu³⁺; and the ionic bonding in lanthanide containing compounds as pure electrostatic attraction. The 7F₁ level splitting was satisfactorily predicted in both cases by very similar sets of charge factors. This similarity indicates that the lanthanide ion treats the chemical species (N, O and F) in its first neighbourhood merely as negative charges.

Share Article



15. Optical properties and electrical resistivity of boron-doped ZnO thin films grown by sol-gel dip-coating method

October 2013

Soaram Kim | Hyunsik Yoon | Do Yeob Kim | Sung-O Kim | Jae-Young Leem

Abstract: Sol-gel dip-coating was used to grow ZnO thin films doped with various concentrations of B ranging from 0 to 2.5at.% on quartz substrates. The effects of B doping on the absorption coefficient (α), optical band gap (E_g), Urbach energy (EU), refractive index (n), refractive index at infinite wavelength (n[∞]), extinction coefficient (k), single-oscillator energy (E_o), dispersion energy (E_d), average oscillator strength (So), average oscillator wavelength (λ_o), moments M⁻¹ and M⁻³, dielectric constant (ε), optical conductivity (σ), and electrical resistivity (ρ) of the BZO thin films were investigated. The transmittance spectra of the ZnO and BZO thin films show that the transmittance of the BZO thin films was significantly higher than that of the ZnO thin films in the visible region of the spectrum and that the absorption edge of the BZO thin films was blue-shifted. The BZO thin films exhibited higher E_g, EU, and E_o and lower E_d, λ_o, M⁻¹ and M⁻³ moments, So, n[∞], and ρ than the ZnO thin films.

Share Article



16. Synthesis and luminescence properties of blue-emitting phosphor K₂Ca₂Si₂O₇:Ce³⁺

January 2014

Yi Luo | Zhiguo Xia | Haikun Liu | Ying He

Abstract: A novel blue-emitting phosphor K₂Ca₂Si₂O₇:Ce³⁺ has been synthesized via a solid-state reaction. The pure phase structure of K₂Ca₂Si₂O₇:Ce³⁺ phosphor was investigated by using the XRD technique and Rietveld refinement. K₂Ca_{1.98}Si₂O₇:0.02Ce³⁺ phosphor exhibited broad-band blue emission peaking at 413nm upon 291nm excitation and 423nm upon 338nm excitation. The critical quenching concentration of Ce³⁺ was determined about 2mol% and the corresponding concentration quenching mechanism was considered to be the dipole-dipole interaction. The double-exponential fluorescence decay curve was also discussed to verify the two kinds of Ce³⁺ centre in K₂Ca₂Si₂O₇ host.

Share Article



17. Synthesis and properties of transparent cycloaliphatic epoxy-silicone resins for optoelectronic devices packaging

January 2013

Nan Gao | WeiQu Liu | ZhenLong Yan | ZhengFang Wang

Abstract: Cycloaliphatic epoxy-silicone resins were successfully synthesized through a two-step reaction route: (i) hydrosilylation of 1,3,5,7-tetramethylcyclotetrasiloxane (TMCTS) and 1,2-epoxy-4-vinyl-cyclohexane (VCMX), (ii) blocking of unreacted SiH in (i) with n-butanol. The molecular structures of the cycloaliphatic epoxy-silicone resins were characterized by Fourier transform infrared (FT-IR) and nuclear magnetic resonance (1H NMR and 29Si NMR). High grafting efficiencies of epoxy groups were confirmed by 1H NMR combined with weighting results, indicating over 90mol% of cycloaliphatic epoxy were grafted on the silicone resins. Subsequently, SiH groups from TMCTS were almost totally consumed after the blocking reactions. In comparison with commercial available cycloaliphatic epoxy resin 3,4-epoxycyclohexylmethyl-3,4-epoxycyclohexanecarboxylate (ERL-4221) cured by MHPA, the cured cycloaliphatic epoxy-silicone resins exhibited better thermal stability, lower water absorption and higher UV/thermal resistance. Moreover, the characteristics of transmittance (>90%, 800nm), 5wt.% mass loss temperature (>330°C) and no yellowing during thermal aging at 120°C or UV aging for 288h of the cured cycloaliphatic epoxy-silicone resins, made them possible for power light-emitting diode (LED) encapsulants, or other packaging materials, like optical lenses, and electronic sealings.

Share Article



18. Sol-gel glasses with enhanced luminescence of laser dye Rhodamine B due to plasmonic coupling by copper nanoparticles

Available online 8 December 2013

Renata Reisfeld | Marek Grinberg | Viktoria Levchenko | Benedykt Kukliński | Sebastian Mahlik | Shlomo Magdassi | Michael Grouchko

Abstract: We present the possibility to increase the emission of Rhodamine B (Rh B) as a result of its interaction with surface plasmons (SF) created by copper nanoparticles (Cu NPs). The optical absorption and emission of Rh B with Cu NPs incorporated into glass films formed by sol-gel method were studied by steady state and picosecond spectroscopy. The observed increased luminescence is the result of interaction of the excited state of the dye with scattered light created by copper plasmons and possible energy transfer from the excited Cu NPs which occur at femtosecond time range. The steady state absorption, excitation, fluorescence and lifetimes excited by picosecond pulses were measured. The quantum efficiencies of the films were obtained by comparative method.

Share Article



19. Synthesis, crystal structures and third-order nonlinear optical properties in the near-IR range of two novel Ni(II) complexes

January 2014

Yanqiu Liu | Hui Wang | Jun Zhang | Shengli Li | Chuankui Wang | Hongjuan Ding | Jieying Wu | Yupeng Tian

Abstract: Two novel Nickel(II) complexes (NiL21 and NiL22) with remarkable two-photon absorption (TPA) and optical power limiting (OPL) properties were synthesized and fully characterized. Single crystals were obtained and solved by X-ray diffraction analysis. Their photophysical properties had been further investigated both experimentally and theoretically. The third-order nonlinear optical (NLO) properties (TPA and OPL) were investigated by open/closed aperture Z-scan measurements using femtosecond pulse laser in the range from 680 to 1080nm. The results revealed that the two Nickel(II) complexes exhibited strong two-photon absorption and superior optical power limiting properties, which are much better than that of the free ligands.

Share Article



20. Transparent and UV-shielding ZnO@PMMA nanocomposite films

December 2013

Yewei Zhang | Shendong Zhuang | Xiaoyong Xu | Jingguo Hu

Abstract: We fabricated successfully the visible light (VL)-traversing and ultraviolet (UV)-shielding zinc oxide quantum dots (ZnO QDs)-poly(methyl methacrylate) (PMMA) nanocomposite films by incorporating suitable UV-absorbing ZnO QDs into a transparent PMMA matrix. The ZnO QDs of about 5nm were first synthesized via a sol-gel route. Then the 3-(trimethoxysilyl)propylmethacrylate (TPM) as a coupling agent is bound to the surface of ZnO QDs, inhibiting the agglomeration of QDs and promoting the compatibility between ZnO QDs and PMMA matrix. Such the transparent ZnO@PMMA nanocomposite films exhibit the prominent UV-absorbing capability and the high optical transparency in the visible-wavelength region, thus have direct practical applications such as UV-shielding windows and glasses.

Share Article



21. Large-area inverse opal structures in a bulk chalcogenide glass by spin-coating and thin-film transfer

December 2013

T. Kohoutek | J. Orava | L. Strizik | T. Wagner | A.L. Greer | M. Bardosova | H. Fudouzi

Abstract: Large (cm²), uniform-thickness areas of an inverse-opal photonic crystal and an inverse-opal monolayer were fabricated in a high-refractive-index As₃₀S₇₀ chalcogenide glass. We have developed an effective low-cost, solution-based process for fabrication of photonic structures in chalcogenide glass from silica-colloidal-crystal thin-film templates (multi- and monolayer). The chalcogenide-glass solution is spin-coated over the silica-opal film template and the infilled composite structure (chalcogenide/opal) is then lifted-off and transferred onto the chalcogenide-glass disc at 225°C, followed by removal of the template in hydrofluoric acid. The extra step introduced in this work (lift-off and transfer) allows a reproducible and large-area structure to be fabricated on a bulk chalcogenide glass. Complete infilling of the silica template is possible due to the nano-colloidal nature (particle size 2–8nm) of the chalcogenide-glass solution and effective solvent release from the spin-coated chalcogenide film during post-annealing. The resulting chalcogenide-glass inverse-opal multilayer exhibits a Bragg peak at 670nm with a reflectance 70%, while the inverse-opal monolayer shows anti-reflectance behaviour <2% in the near-infrared region (1215–1660nm).

Share Article



22. Comparison of parameters of q-switching saturable absorbers estimated by different models and the impact of accuracy of input data on the results of the estimation

March 2014

J. Młyńczak | K. Kopczyński

Abstract: Descriptions of the main classical models used to estimate the principal parameters of q-switching saturable absorbers are presented. On the basis of these models comparative analysis of q-switching saturable absorbers was done and the best one chosen. Additionally the impact of the accurate determination of the input data such as transmission, thickness and refractive index on the principal parameters was analysed. In order that the results of this analysis are useful not only from theoretical but also from practical point of view a complete setup for investigation of saturation of absorbers was built and investigations of three types of q-switching saturable absorbers Cr⁴⁺:YAG, V³⁺:YAG and Co²⁺:YAG were carried out. According to the knowledge of the authors the principal parameters of Co²⁺:YAG saturable absorber at 1.33 μ m wavelength are presented herein for the first time.

Share Article



23. Femtosecond laser writing over silver nanoparticles system embedded in silica using nonlinear microscopy

January 2014

Jacob Licea-Rodríguez | Israel Rocha-Mendoza | Raúl Rangel-Rojo | Luis Rodríguez-Fernández | Alicia Oliver

Abstract: We present results for the induction and monitoring of structural modification of a composite consisting of elongated silver nanoparticles films embedded in silica using ultrafast femtosecond laser irradiation and second harmonic generation imaging, respectively. Waveguide-like patterns are written and characterized under a laser scanning nonlinear microscope system by simply changing the laser fluence in the sample; switching in this way between two different physical processes occurring only within the composite film: second harmonic generation and laser induced nanoparticles removal. A study of the nanoparticles damage process as a function of the laser energy, polarization and scan velocity is also presented and discussed. The use of the non-irradiated zone between two written channels is proposed as a potential linear and nonlinear optical waveguide.

Share Article



24. Synthesis of ZnO nanorod and the annealing effect on its photoluminescence property

March 2006

Lili Wu | Youshi Wu | Xiaoru Pan | Fanyuan Kong

Abstract: Single crystal ZnO nanorod has been prepared by hydrothermal method. Optical properties of the nanorod were studied by annealing the nanorod at different ambiances. The annealed and unannealed samples were characterized by X-ray diffraction (XRD), transmission electron microscopy (TEM), X-ray photoelectron spectroscopy (XPS) and Fourier transform infrared spectroscopy (FTIR), UV-Vis absorption (UV) spectroscopy and photoluminescence (PL) spectroscopy. The photoluminescence spectra under excitation 325nm for the as-prepared ZnO nanorod show three bands: UV emission at 386nm, blue emission at 468 and orange emission at 640nm. By annealing the crystals in ammonia gas at 600°C, the PL spectra shows obvious UV near band-edge emission at 386nm and a green emission at 510nm. While annealing the crystals in air, the orange emission was greatly enhanced.

Share Article



25. Structural, FTIR and photoluminescence studies of Cu doped ZnO nanopowders by co-precipitation method

September 2012

S. Muthukumaran | R. Gopalakrishnan

Abstract: Cu doped ZnO (Zn_{1-x}Cu_xO, x=0, 0.02, 0.04 and 0.06) nanopowders have been synthesized by co-precipitation method and annealed at 500°C for 2h under Ar atmosphere. The synthesized samples have been characterized by powder X-ray diffraction, energy-dispersive analysis X-ray (EDAX) spectra, UV-Visible spectrophotometer and Fourier transform infrared (FTIR) spectroscopy. The XRD measurement reveals that the prepared nanoparticles have different microstructure without changing a hexagonal wurtzite structure. The calculated average crystalline size decreases from 22.24 to 15.93nm for x=0 to 0.04 then reaches 26.54nm for x=0.06 which is confirmed by SEM micrographs. The change in lattice parameters, micro-strain, a small shift and broadening in XRD peaks and the reduction in the energy gap from 3.49 to 3.43eV reveals the substitution of Cu²⁺ ions into the ZnO lattice. Hydrogenation effect improves the crystal quality and optical properties. It is proposed that Cu doping concentration limit is below 6% (0.06) molar fraction which is supported by the detailed XRD analysis and the derived structural parameters. This Cu concentration limit was proposed as below 5% by previous studies. The presence of functional groups and the chemical bonding is confirmed by FTIR spectra. PL spectra of the Zn_{1-x}Cu_xO system show that the shift in near band edge (NBE) UV emission from 398 to 403nm and a shift in green band (GB) emission from 527 to 522nm which confirms the substitution of Cu into the ZnO lattice.

Share Article



Share this page:




ADVERTISEMENT

materialstoday
webinar

A new frontier in coatings analysis: free online event

29 April 2014
4.00pm (BST)
5.00pm (CEST)
11.00am (EDT)



REGISTER NOW

- | | | | | | | |
|-------------------------------------|---|---|--|-------------------------------------|---|---------------------------|
| Readers | Authors | Librarians | Editors | Reviewers | Advertisers/ Sponsors | Societies |
| View Articles | Author Information Pack | Ordering Information and Dispatch Dates | Publishing Ethics Resource Kit | Reviewer Guidelines | Advertisers Media Information | |
| Volume/ Issue Alert | Submit Your Paper | Abstracting/ Indexing | EES Support | Log in as Reviewer | | |
| | Track Your Paper | | Guest Editors | | | |
| | Webshop | | | | | |



[Choose language ▼](#)

[Industries](#)

[Advertising](#)

[Careers](#)

[Feedback](#)

[Site Map](#)

[Elsevier Websites](#)

[A Reed Elsevier Company](#)

Copyright © 2014 Elsevier B.V. All rights reserved.

[Privacy Policy](#)

[Terms & Conditions](#)

Cookies are set by this site. To decline them or learn more, visit our [Cookies](#) page.